

PREPARATION, CHARACTERIZATION AND STUDIED BIOLOGICAL EFFECT AS ANTIOXIDANT OF NEW LIGAND COMPLEXES OF IONS (CO (II), NI (II), CU (II), CD (II), HG (II), AG (I), AU (III) DERIVED FROM AZO COMPOUND

Zainab Ghanim Abd^{a,*}, Layla Ali Mohammed^b

^a Department of Chemistry, College of Education for Girls, University of Kufa, Iraq

^b Department of Chemistry, College of Education for Girls, University of Kufa, Iraq

Abstract: A number of Co (II), Ni (II), Cu (II), Cd (II), Au (III), and Ag (I) ligand complexes were synthesized and studied. Using 4-aminobenzonitrile and 4-methylimidazole, a novel azo ligand was designed. Mass spectra, electronic spectroscopy, molar conductance, elemental analysis (C.H.N.), magnetic measurements, ¹HNMR, IR spectral investigations, and electronic spectroscopy were among the analytical techniques used to study ligand structure and their transitional metal complexes. [M(L)2Cl2] is the composition of these complexes, according to the data, where M stands for Co (II), Ni (II), Cu (II), Cd (II), and Hg (II). When M=Au (III), [MLCl2] Cl. Where M=Ag(I), we have [MLH2OCl]. A tetra hydra geometry is indicated by Ag(I) and a square planar geometry by Au (III) complex, respectively, while all other complexes have an octahedral geometry according to the complexes' electronic spectrum data and magnetic susceptibility. According to the IR data, the furthest azo nitrogen atom and the imidazole nitrogen atom serve as the co-ordination sites. The behavior of Azo ligand is bidentate. DPPH radical scavenging activity was demonstrated by the compound Au (III). The compound exhibits prospective and promising antioxidant actions, according to the results overall. Gold's anticancer properties with great efficacy, the au-complex destroys lung cancer cells while having no effect on healthy cells. This is a significant finding about the application of a gold complex as a very focused lung cancer treatment.

Keywords: new ligand complexes, azo ligand, antioxidants, anticancer.

1. Introduction

The azo dyes are commonly studied in coordination chemistry due to their easy synthesis, availability, and electronic properties. They have also shown potential in pharmaceutical and analytical fields. Azo compounds, which contain the (-N=N-) group, have gained importance in inorganic chemistry [1,3]. These compounds are highly significant due to their unshared electron pair on the nitrogen atom and their effectiveness and derivatives [4]. They have a high affinity for metal ions, forming stable chelated complexes with five- or six-membered rings [1] Azo compounds are a class of chemical compounds that have been used as dyes and pigments for a long time and continue to attract interest in scientific research [5]. Both synthetic and natural azo molecules are important sources for drug prototypes and drug discovery. Azo dyes are significant organic chemicals due to their simple synthesis and stability; they have various applications in industries such as textiles, printing inks, paper, drugs, and food coloring [6]. Azo compounds also exhibit biological activities such as anticancer [7], antioxidant[8,9], anti-bacterial[10], and protein synthesis, as

well as inhibiting RNA and DNA[11]. Many Azo compounds have been studied as ligands in complexes and have shown effectiveness in treating conditions such as inflammation, tuberculosis, infections, and diabetes [12,13] **In this research paper, an azo ligand derived from (4-aminobenzonitrile and 4-methyl-1H-imidazole) was prepared. Some metal complexes were prepared from it, and the gold complex was used for its biological activity as an antioxidant and anticancer agent for lung cancer.**

2. Experimental and Materials

Without additional purification, all chemicals were used; they were provided by BHD, Sigma Aldrich, A.K. Scie, and Fluka. The ligand and its complexes' melting points were determined using the electro-thermal melting point model 9300. The micro analytical unit of the 1180 C.H.N elemental analyzer was used to perform elemental analyses. On a Shimadzu twin beam model 1700 ultraviolet-visible (UV-Vis) spectrophotometer, electronic spectra were captured. Utilizing a Shimadzu model 8400 FTIR spectrophotometer, fourier-transform infrared (FTIR) spectra in the 4000-400/cm wave number range were recorded on a KBr disc. Dimethyl sulfoxide-d₆ (DMSO-d₆) was used as the solvent, and a Bruker Ultra Shield 3000 MHz apparatus from Switzerland was used to record proton nuclear magnetic resonance (1H-NMR) spectra in ppm units. Mass spectra in the mass range of m/z 5-2000 in quad mode and 50-1700 in linear ion trap mode were acquired using an AB Sciex 3200 QTRAP LC/MS/MS. Using a balance magnetic MSB-MKI, magnetic susceptibility measurements were performed, and Pascal's constants were used to account for diamagnetic effects.

2.1. preparation of Azo Ligand

The method previously outlined [14] Scheme 1 was used to prepare this heterocyclic azo ligand. A transparent solution was achieved by whisking a solution of 1.18 g of 4-aminobenzonitrile (0.01 mol) in 80 mL of water and 2 mL of strong HCl (37%). The solution was then cooled down between 0 and 5 degrees Celsius. Drop by drop, while keeping the temperature below 5 degrees Celsius, a solution of sodium nitrite (0.71 g, 0.01 mol) in 10 mL of water was added. After stirring the liquid for 20 minutes in an ice bath, urea was added to eliminate any remaining nitrite. The coupling component 4-methyl-1H-imidazole (0.82 g, 0.01 mol) was dissolved in 200 mL of cooled alkaline ethanol at 5°C and added to the resultant diazonium chloride solution. The solution was acidified to a pH of 7 using diluted hydrochloric acid after being refrigerated for a full day. After being cleaned and filtered multiple times with distilled water, the orange precipitate was allowed to dry naturally before being re-crystallized twice using heated ethanol. Ultimately, it was dried at 60°C in an oven. Table 1 contains a tabulation of some analytical and physical data for this azo dye. The azo ligand preparation procedures are depicted in Scheme 1.

2.3. Antioxidant activity

Using the 1,1-diphenyl-2-picrylhydrazyl (DPPH) test technique, the synthetic compounds' ability to scavenge free radicals in vitro was assessed [15,16]. The medication was first dissolved in methanol to a stock solution that was diluted to different quantities (50-200 mg/mL). Subsequently, a 0.003% (w/v) methanol solution of DPPH (1 mL) was mixed with a 2 mL methanolic solution of the produced compounds. After giving the mixture a good shake, it was left to stand for half an hour. The absorbance at 517 nm was determined, and the scavenging activity percentage was computed. Ascorbic acid was employed as a standard. Using the formula $I\% = (Ac-As)/Ac \times 100$, where Ac is the absorbance of the control and as is the absorbance of the sample, the inhibition ratio (I%) of the investigated substances was calculated.

2.4. Methods

The A549 human lung cancer cell line and HdFn non-malignant cells were obtained from the National Cell Bank of Iran (Pasteur Institute, Iran). The cells were grown in RPMI-1640 (Gibco) and DMEM: F12 medium (Gibco), respectively, supplemented with 10% FBS (Gibco) and antibiotics (100 U/ml penicillin and 100 µg/ml streptomycin). The cells were maintained at (37 °C) in a humidified atmosphere with (5% CO₂) and were passaged using trypsin/EDTA (Gibco) and phosphate-buffered saline (PBS) solution. The same media and conditions were used for both monolayer and 3D colony cell cultures. MTT cell viability assay: Cell growth and viability were assessed using the MTT [3-(4,5-dimethylthiazol-2-yl)-2,5-diphenyltetrazolium bromide] (Sigma-Aldrich) assay. For monolayer cultures, cells were digested with trypsin, harvested, and seeded at a density of (1.4×10^4 cells/well) in (96-well plates) with (200 µl) of fresh medium per well for (24 hours). Once the cells formed a monolayer, they were treated with (500-100 µg/ml) of the compounds for (24 hours at 37 °C in 5% CO₂). After the treatment, the supernatant was removed and (200 µl/well of MTT solution) (0.5 mg/ml in PBS) was added. The plate was then incubated at (37 °C) for an additional (4 hours). The supernatant was removed and (100 µl) of dimethyl sulfoxide was added to each well. The plate was incubated on a shaker at (37 °C) until the crystals were completely dissolved. Cell viability was measured by absorbance at (570 nm) using an ELISA reader. The concentration of the compounds that resulted in 50% cell death (IC₅₀) was determined from the respective dose-response curves.

3. Results and Discussion

Every ligand compound that was employed in this study was stable in air and easily soluble in ethanol, methanol, DMF, and DMSO. Numerous methods, such as molar conductivities, elemental analysis, magnetic susceptibility, UV-Vis, IR, mass spectra, and ¹H NMR spectra, were used to describe the metal complexes. These analyses' findings agreed well with the outcomes of the trial. Except for the complexes of Au (III) and Ag(I), which had a ratio of 1:1, the majority of complexes were discovered to have a (metal: ligand) ratio of (1:2). With the exception of the Ag(I) complex and the Au (III) complex, which displayed tetrahedral and square planar molecular geometries, the room temperature magnetic susceptibilities of the chelate complexes revealed an octahedral molecular geometry. Low conductivity values were seen in the majority of the produced chelate complexes, suggesting that they were not electrolytic in origin. The Au (III) complex, on the other hand, displayed greater conductivity values, indicating an electrolytic character. With the exception of the Au (III) and Ag(I) complexes, the

results of the micro-element analyses for the complexes showed good agreement with the theoretical values. The TLC technique and elemental analysis of C, H, and N were used to test the ligand's purity.

Table 2. shows the results of the elemental micro-analysis for the ligand and complexes.

3.2. Mass spectra

The synthesized Ligands' mass spectra were recorded at room temperature. By locating the molecular ion peaks, the suggested formula for the produced compounds was verified. The suggested formula for the chemical (C₁₁H₉N₅) is confirmed by the mass spectra of the Azo Ligand (L), which displayed a peak for the molecular ion at m/z 211 (3.28%). Confirming the suggested formula, the mass spectra of the nickel complex also revealed a peak for the molecular ion at m/z 551.6 (0.8%), which corresponds to the combination Ni(C₂₂H₁₈N₁₀) Cl₂.

No.	Compound	Chemical formula	M.wt	C Found % (cal.)	H Found % (cal.)	N Found % (cal.)	M Found % (cal.)
1	L	C ₁₁ H ₉ N ₅	211.2	62.5	4.29)(4.28	33.15	-----
2	[Co(L) ₂ Cl ₂]	C ₂₂ H ₁₈ N ₁₀ Ni Cl ₂	552.33	47.79 (47.86)	3.25 (3.27)	25.34 (25.40)	10.66 (10.75)
3	[Ni(L) ₂ Cl ₂]	C ₂₂ H ₁₈ N ₁₀ CoCl ₂	552.09	47.81 47.9)(3.26 (3.29)	25.32 (25.54)	11.24 (11.30)
4	[Cu(L) ₂ Cl ₂]	C ₂₂ H ₁₈ N ₁₀ CuCl ₂	556.9	44.71 (44.74)	3.23)((3.25)	25.13 (25.24)	11.48 (11.67)
5	[Ag(L) Cl.H ₂ O]	C ₁₁ H ₁₁ ON ₅ AgCl	372.56	35.43 (35.75)	2.95 (2.98)	18.78 (18.89)	28.95 (29.03)
6	[Hg(L) ₂ Cl ₂]	C ₂₂ H ₁₈ N ₁₀ HgCl ₂	693.99	35.44 (35.49)	2.59 (2.62)	20.17 (20.32)	28.90 (28.97)
7	[Cd(L) ₂ Cl ₂]	C ₂₂ H ₁₈ N ₁₀ CdCl ₂	605.81	40.60 (41.02)	2.97 (2.99)	23.10 (23.23)	18.55 (18.72)
8	[Au(L)Cl ₂] Cl	C ₁₁ H ₉ N ₅ AuCl ₃	514.46	25.65 (25.70)	1.74 (1.79)	13.60 (13.66)	38.29 38.39)(

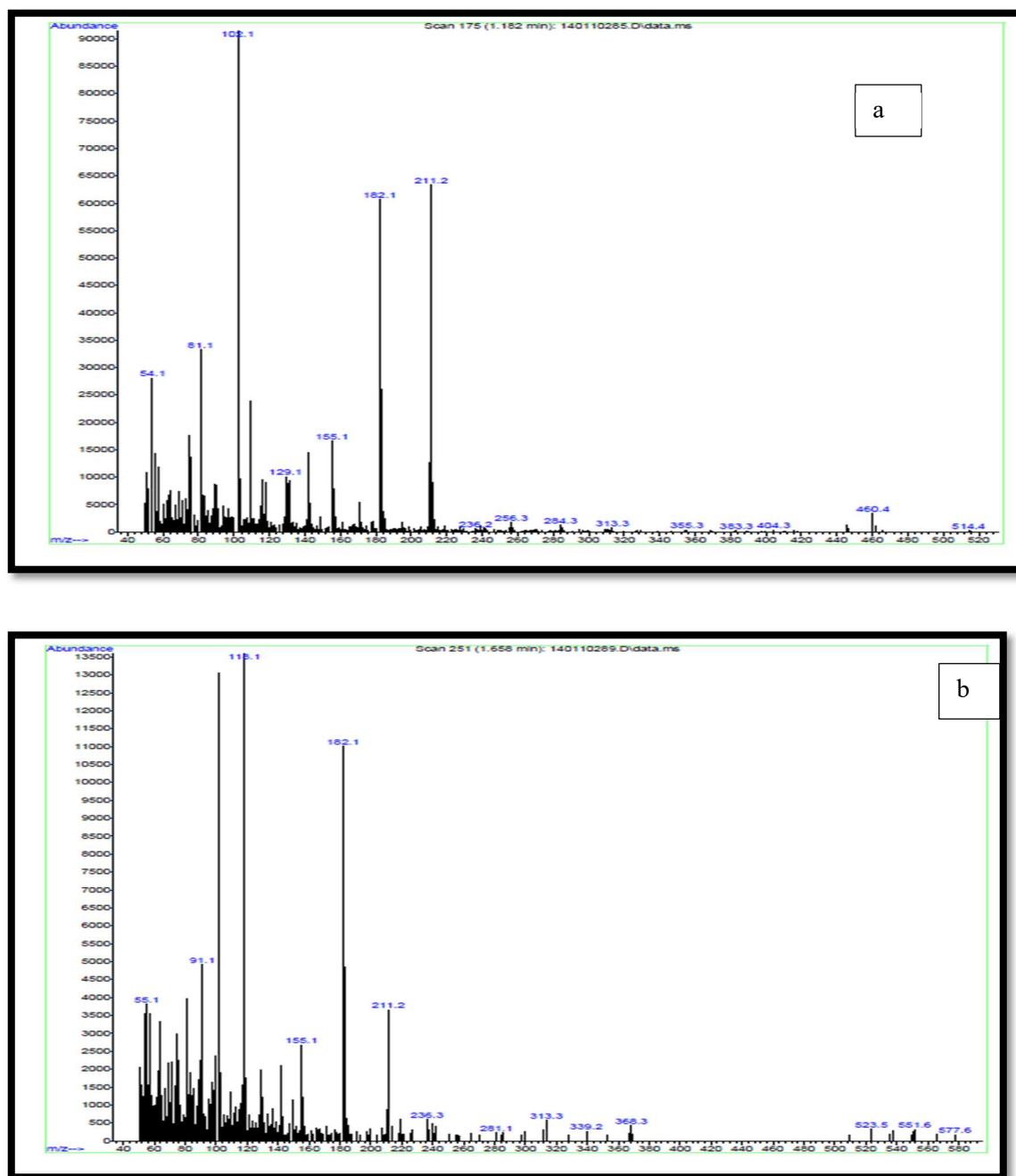
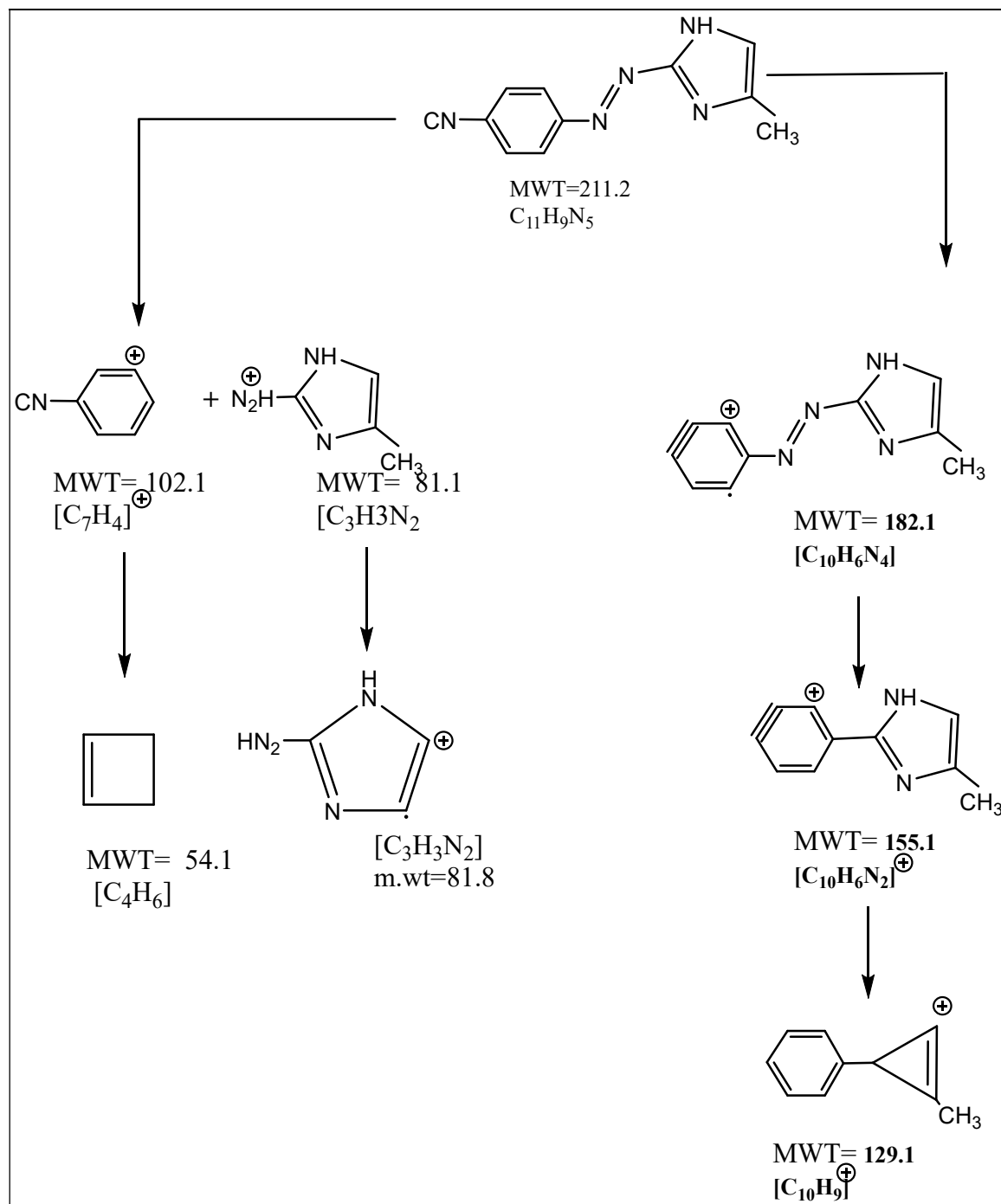


Fig 1. (a) Mass spectra of the azo-ligand, **(b)** Mass spectra of the Ni(II) complex



Scheme 2. Fragment of Azo ligand

Scheme 3. Fragment of Ni (II) Complexes

3.3¹H NMR Spectra of azo- ligand

The ¹H NMR spectrum of this compound was recorded using DMSO-d₆ as the solvent. The singlet signal at δ 2.5 ppm can be attributed to the solvent protons. The aromatic protons appeared as multiple signals in the range of δ (6.1-8.1) ppm. The CH₃ group in the imidazole ring was observed at 2.2 ppm, while another signal at δ 13.2 ppm was assigned to the imidazole (-NH-) proton. Additionally, a signal

a

b

Fig 2. The ^1H NMR spectrum of (a) ligand and (b) Cd complex

3.4. Infrared spectra

The infrared spectra of the complexes and the free ligand were compared in order to identify any potential alterations that might have happened during complexation. Table 3 is a list of all the data. In all metal complexes, the bands corresponding to the azomethine group ($C=N$) in azo ligands were shifted to a lower frequency and seen at (1635 cm^{-1}). This suggests that the azomethine group's nitrogen atom participates in coordination [16]. Furthermore, a band at (1426 cm^{-1}) was seen in the azo ligand, and this band can be assigned to the ($N=N$) group. This band was also shifted to a lower frequency in the metal complexes, further indicating the participation of the nitrogen atom of the azo group in coordination [17]. The presence of coordinated water molecules in the Ag(I) complex was observed by broad bands around (3600 cm^{-1}), which were further confirmed by bands at ($765\text{--}780\text{ cm}^{-1}$). The IR spectra of all complexes also showed new bands at approximately ($503\text{--}518\text{ cm}^{-1}$), which were assigned to $\nu(M-N)$. A representative example of these spectra is given in (Fig. 3).

Table 3. lists the characteristic IR frequencies (in cm^{-1}) of the ligand and complexes.

Compound	N-H	$\nu(C=C)$	$\nu(C=N)$ imidazole	$\nu(N=N)$	$(C\equiv N)\ \nu$	$\nu(M-N)$
L	3442	1598	1635	1426	2223	-----
$[Co(L)_2Cl_2]$	3406	1600	1615	1417	2225	509
$[Ni(L)_2Cl_2]$	3415	1600	1624	1415	2229	505
$[Cu(L)_2Cl_2]$	3433	1598	1598	1415	2225	511
$[Ag(L)Cl.H_2O]$	3493	1600	1624	1419	2225	505
$[Au(L)Cl_2]Cl$	3493	1604	1625	1402	2227	503
$[Cd(L)_2Cl_2]$	3423	1597	1624	1417	2227	505
$[Hg(L)_2Cl_2]$	3417	1598	1624	1421	2225	518

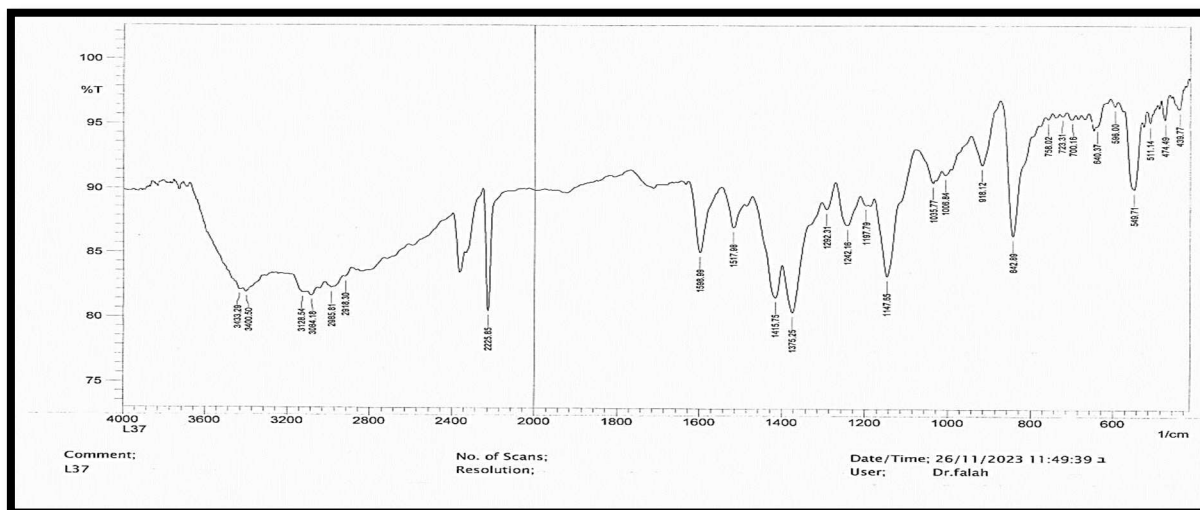
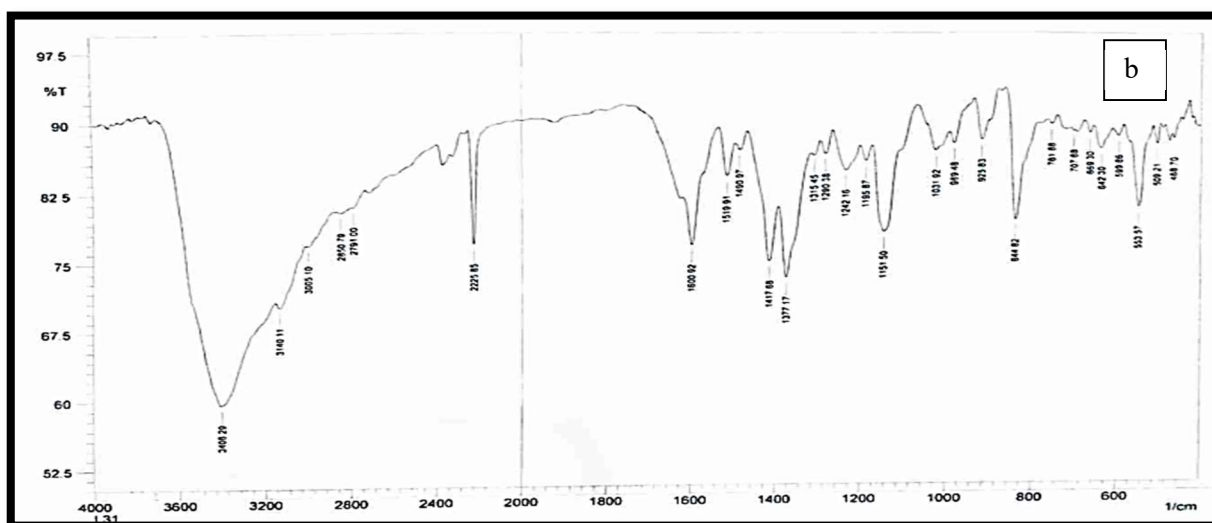
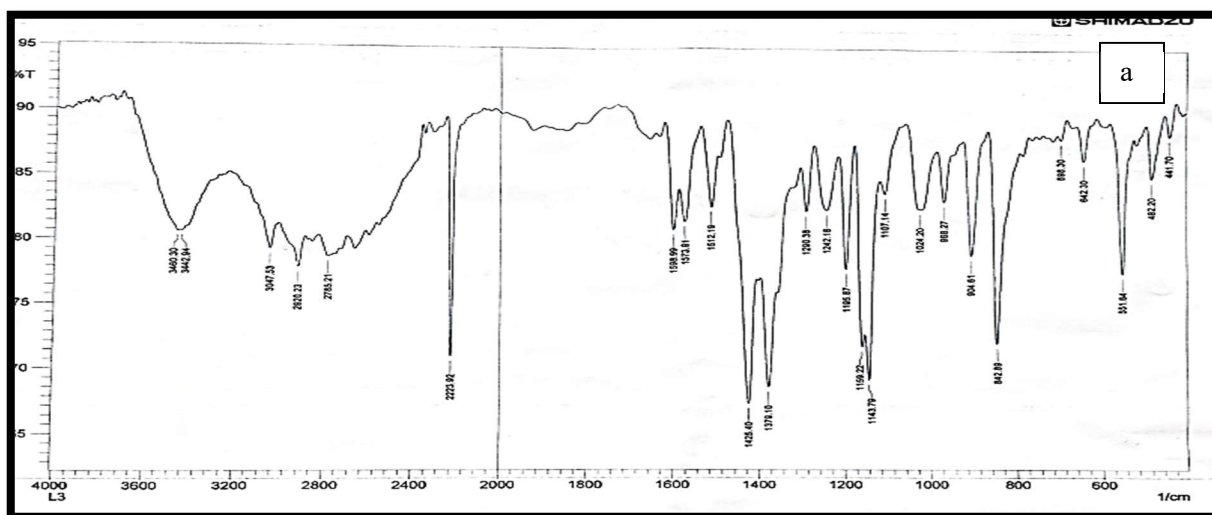
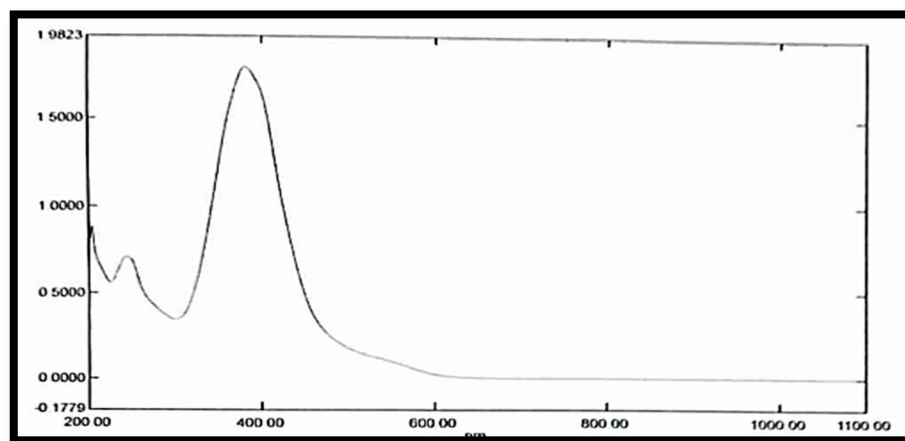


Fig 3. IR- spectrum of (a) azo ligand, (b)Ni (II) Complex, (C) Cu (II) complex**3.5. Electronic Spectra:**

Electronic spectra provide detailed information about the electronic structure. The UV-Vis spectrum of the (azo) ligand exhibits two charge transfer (CT) bands at 245nm (40816 cm⁻¹) and 382nm (26178cm⁻¹), attributed to $\pi \rightarrow \pi^*$ and $n \rightarrow \pi^*$ transitions within the (azo) ligand. The band observed at 382nm in the spectrum of the free ligand is red-shifted to 451-618nm in complexes due to ligand to metal charge transfer (LMCT) transition (17,18) suggesting an octahedral geometry around the metal (II) in the complexes. The electronic transitions, magnetic properties, and conductivity values of the ligand and its complexes are listed in Table 4 and shown in (Fig. 4).

Table 4. Electronic spectra of complexes

Compound	λ (nm)	ν (cm ⁻¹)	Transition	Geometry	Hybridization
L	245	40816	$\pi \rightarrow \pi^*$	-----	-----
	382	26178	$n \rightarrow \pi^*$		
(Co(L) ₂ Cl ₂)	468	21367	M \rightarrow L,CT	Octahedral	sp ³ d ²
[Ni(L) ₂ Cl ₂]	465	21505	M \rightarrow L,CT	Octahedral	sp ³ d ²
[Cu(L) ₂ Cl ₂]	495	20202	M \rightarrow L,CT	Octahedral	sp ³ d ²
(Zn(L) ₂ Cl ₂)	451	22172	M \rightarrow L,CT	Octahedral	sp ³ d ²
(Cd(L) ₂ Cl ₂)	468	21367	M \rightarrow L,CT	Octahedral	sp ³ d ²
(Hg(L) ₂ Cl ₂)	462	21645	M \rightarrow L,CT	Octahedral	sp ³ d ²
(AgLCIH ₂ O)	483	20703	M \rightarrow L,CT	Tetrahedral	SP ³
[AuLCl ₂]Cl	618	16181	M \rightarrow L,CT	Square planer	dSP ²



a

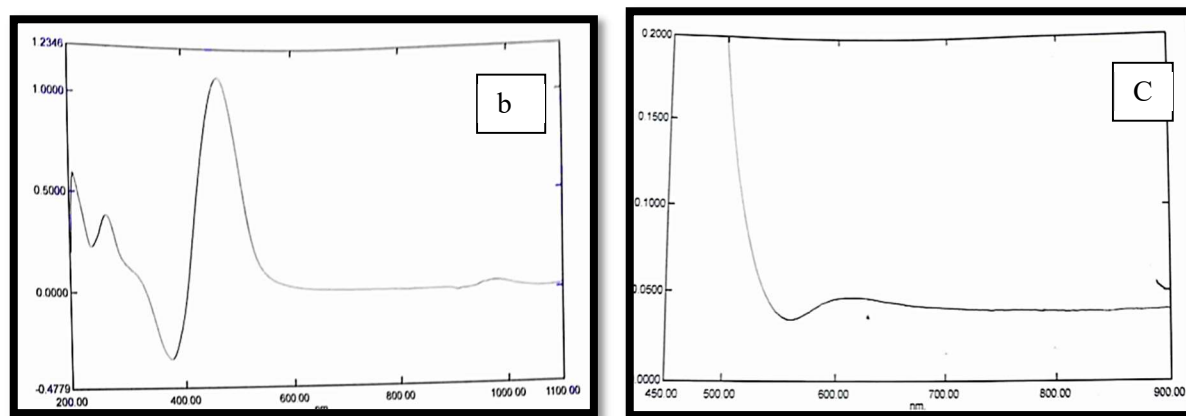
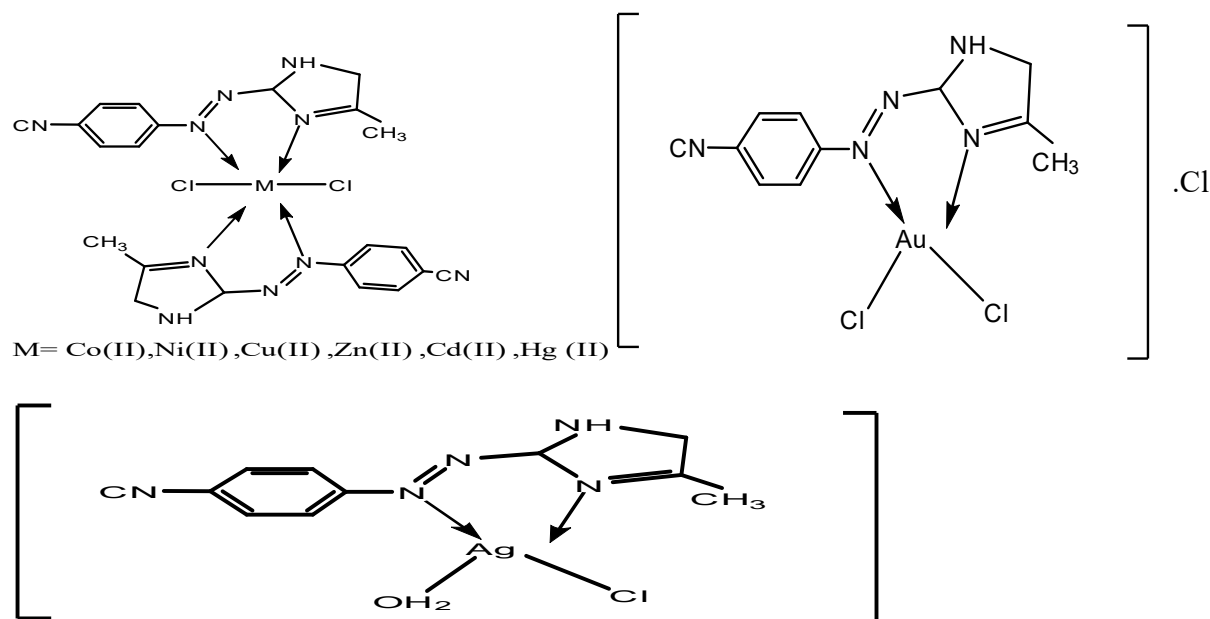


Fig 4. The spectra of electronic: (a) azo ligand & (b)Ni (II) complex (c) Au(III) complex

3.6. Measurement of conductivity

Molar conductance (Λ_m) measurements were performed on the metal complexes in ethanol solvent at a concentration of 10^{-3} M and room temperature. The prepared chelate complexes showed a range of conductivity values between ($2.3-11.6 \text{ s.mol}^{-1}.\text{cm}^2$), indicating that they are non-electrolytes and non-conductive [19]. However, the molar conductance of the Au (III) complex was ($35 \text{ s.mol}^{-1}.\text{cm}^2$), indicating that it is an electrolyte with a (1:1 electrolyte ratio) a [20]. This information can be used to determine the structures of the complexes.



Scheme 4. the proposed structural formula of the complexes

3.7. Antioxidant screening (DPPH radical scavenging activity)

Table 5 and Figure 5 display the scavenging activity data of a few synthesized substances. In laboratories, the DPPH assay is frequently employed to assess the potency of antioxidants. The absorption peak of DPPH is located at 517 nm, and it vanishes when it is reduced by an antioxidant or turns into a radical. The hue of this diamagnetic molecule changes from purple to yellow because it is stable. This shift in hue serves as a gauge for the tested compounds' capacity to donate hydrogen. When antioxidants combine with DPPH, 1,1-diphenyl-2-picrylhydrazine is produced. The compounds were tested for their scavenging potential by interacting for 30 minutes at five different concentrations with stable free-standing DPPH. The maximum scavenging activity was demonstrated by the complex Au (III), most likely as a result of the azo group. Usually deactivating aromatic rings, electron-withdrawing substituents are unable to bind free radicals. When comparing the synthesized complex Au (III) compounds to common antioxidants such as ascorbic acid, which is used as a reference in the search for their antioxidant activity using the stable free radical approach [20], the findings of the antioxidant activity evaluation demonstrated that all the compounds had antioxidant capabilities.

Table 5. Scavenging activity of some synthetic compound

Conc. ($\mu\text{g/ml}$)	Ascorbic acid		Au (III)	
	mean	SD	Mean	SD
200	82.716	2.7783	79.051	1.66937
100	74.80733	1.446881	65.74033	1.00228
50	64.313	3.142829	54.47533	2.695338
25	52.73933	3.183176	40.818	5.208505
12.5	39.275	1.351383	28.974	4.207328

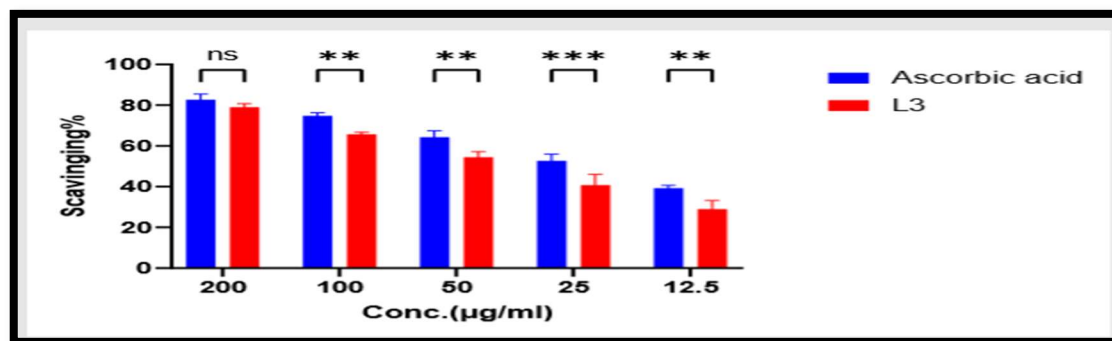


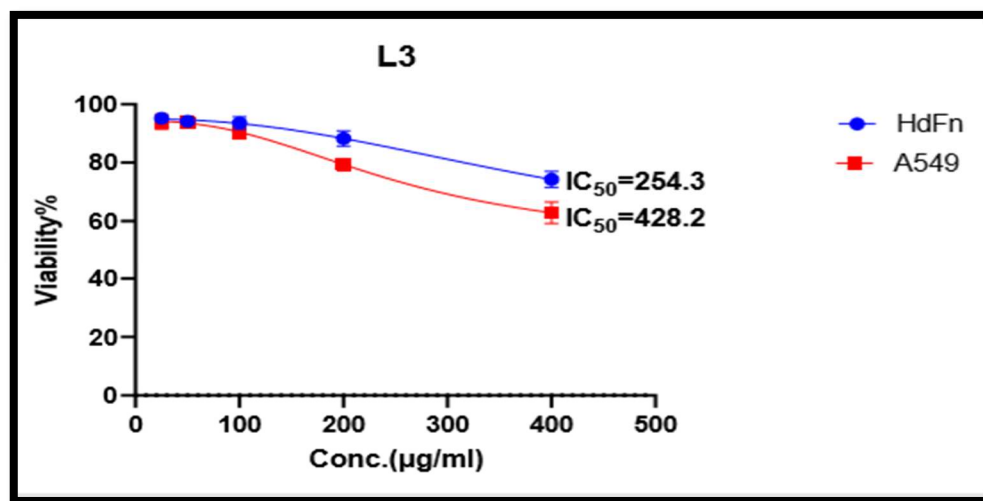
Fig 5. Scavenging activity of the compound using DPPH

3.8. Anticancer activity of gold

At different doses, the cytotoxic activity of gold against the lung cancer (A549) cell line was assessed and contrasted with that of healthy cells. Test concentrations for the anticancer effects of were (25 μg , 50 μg , 100 μg , 200 μg , and 400 μg). as displayed in Table 6 and (Fig. 6). (6). At larger concentrations, gold's anticancer activity grew. Gold displayed encouraging outcomes when compared to healthy cells. Based on prior research, gold's cytotoxic effects may be caused by its physical and chemical interactions with intracellular proteins, phosphate groups in DNA, and nitrogen bases [21].

Table 6 The percentage of inhibition(mean) and SD for the Au (III) complex

L3	HdFn		A549	
Conc.($\mu\text{g/ml}$)	mean	SD	Mean	SD
400	74.26733	2.761597	62.886	3.7041
200	88.27167	2.60934	79.43667	1.596764
100	93.59567	2.100082	90.39333	1.445637
50	94.174	1.571414	93.82733	1.290811
25	95.216	0.820906	94.02033	2.632729

**Fig 6.** Percentage of inhibition in cells of (a) cancer (A549) line cell against the concentration of complex Au (III)(b) normal line cell (HdFn) against the concentration of complex Au (III)

Conclusion

Azo compounds ligand – based metallic complexation has been proven to be a highly remarkable area of research due to its versatile and multidisciplinary application. Specifically, azo compounds complexes in biology have shown tremendous potential as antioxidant and anticancer agents in plenty of chemical synthesis. Because of the capacity of azo compounds to cast complexes with different types of metal ions and their pharmacological properties, these are a relevant class of chemical molecules. azo compounds are considered as very important class of organic compounds because of their ability to form complexes with versatile metal ions such as Co, Ni, Cu, Cd, etc, and of their pharmacological properties. These metal complexes containing azo compounds have been of much interest over the last years, because of their potential application in designing newer therapeutic agents. But still there is need to explore the biological properties of synthesized transition metal complexes and to synthesize newer complexes with more applications. We conclude this study by emphasizing that it is expected that this review presentation will be of real use for inorganic chemistry researchers who are working with azo compounds ligands.

FUNDING

The research did not receive any financial support or funding from grants or external sources.

ETHICS APPROVAL AND CONSENT TO PARTICIPATES

This article does not contain any studies conducted by any authors of this work. This article does not contain any studies involving patients or animals as test objects.

Informed consent was not required for this article.

CONFLICT OF INTEREST

No conflict of interest was declared by the authors.

AUTHOR CONTRIBUTION

Author Layla Ali Mohammed —selected the literature data on the review topic. Author Zainab Ghanim Abd —contributed to manuscript preparation. All authors participated in the discussions.

DATA AVAILABILITY

The data that support the findings of this study are available from the corresponding author upon reasonable request.

References

- 1 Sayqal A, Alotaibi MM, Kassem MA, Ahmed SA. Competence azo dyes sensors of new based fluorophores for spectrophotometric trace determination of cobalt in real water samples. *Arabian Journal of Chemistry*. 2024 Feb;105686. <https://doi.org/10.1016/j.arabjc.2024.105686>.
2. Shalabi, K., Abd El-Lateef, H.M., Hammouda, M.M., Abdelhamid, A.A., *ACS Omega*, 2024, Vol.9, P.18932–18945. <https://doi.org/10.1021/acsomega.3c09072>.
3. Taha Saad S. Synthesis, characterization and theoretical aspects of copper and zinc divalent ion complexes with azo dye derived from 4,5-diphenylimidazole. *Bull Chem Soc Ethiop* [Internet]. 2024 Jan 23;38(2):313–23. Available from: <https://www.ajol.info/index.php/bcse/article/view/263211>
4. Kadagathur M, Patra S, Devabattula G, George J, Phanindranath R, Shaikh AS, et al. Design, synthesis of DNA-interactive 4-thiazolidinone-based indolo-/pyrroloazepinone conjugates as potential cytotoxic and topoisomerase I inhibitors. *Eur J Med Chem*. 2022 Aug 5;238. <https://doi.org/10.1016/j.ejmech.2022.114465>
5. Aljamali DrN, Farhan Z. Anticancer Study of Innovative Macrocyclic Formazan Compounds from Trimethoprim Drug. *Egypt J Chem* [Internet]. 2022 Apr 20;0(0):0–0. Available from: [10.21608/EJCHEM.2022.132514.5852](https://doi.org/10.21608/EJCHEM.2022.132514.5852)

6. Reda MM, Mohammed LA. Preparation, Characterization and studied Biological Effect as Antioxidant of Azo Compound and Schiff base Complexes. Vol. 10, Journal of Survey in Fisheries Sciences. <https://doi.org/10.17762/sfs.v10i3S.123>
7. Al Nasr IS, Koko WS, Khan TA, Gürbüz N, Özdemir I, Hamdi N. Evaluation of Ruthenium(II) N-Heterocyclic Carbene Complexes as Enzymatic Inhibitory Agents with Antioxidant, Antimicrobial, Antiparasitical and Antiproliferative Activity. Molecules. 2023 Feb 1;28(3). [10.3390/molecules28031359](https://doi.org/10.3390/molecules28031359)
8. Moreno-Alcántar G, Picchetti P, Casini A. Gold Complexes in Anticancer Therapy: From New Design Principles to Particle-Based Delivery Systems. Vol. 62, Angewandte Chemie - International Edition. John Wiley and Sons Inc; 2023. <https://doi.org/10.1002/ange.202218000>
9. Shen N, WT, GQ, LS, WL, & JB(). P flavonoids. : Classification, distribution, biosynthesis, and antioxidant activity. . Food Chem. 2022;383, 132531. <https://doi.org/10.1016/j.foodchem.2022.132531>
10. Slassi S, Fix-Tailler A, Larcher G, Amine A, El-Ghayoury A. Imidazole and azo-based schiff bases ligands as highly active antifungal and antioxidant components. Heteroatom Chemistry. 2019;2019. <https://doi.org/10.1155/2019/6862170>
11. Shrivastava R, Gupta P. (E)-N-(4-(2-(N-benzylidene) hydrazine carbonyl)phenyl)pyridine-4-sulfonamide Schiff bases: Synthesis, spectroscopic characterization, thermo gravimetric analysis and antimicrobial activity. Results Chem. 2023 Jan 1;5. <https://doi.org/10.1016/j.rechem.2023.100933>
12. El-Ghamry HA, Al-Ziyadi RO, Alkhatib FM, Takroni KM, Khedr AM. Metal Chelates of Sulfafurazole Azo Dye Derivative: Synthesis, Structure Affirmation, Antimicrobial, Antitumor, DNA Binding, and Molecular Docking Simulation. Bioinorg Chem Appl. 2023;2023. <https://doi.org/10.1155/2023/2239976>
13. Zhao MY, Tang YF, Han GZ. Recent Advances in the Synthesis of Aromatic Azo Compounds. Vol. 28, Molecules. Multidisciplinary Digital Publishing Institute (MDPI); 2023. ; <https://doi.org/10.3390/molecules28186741>
14. Javaid M, Haq IU, Nadeem H, Fatima H, Khan AU, Irshad N. Design, synthesis and screening of indole acetic acid-based tri-azo moieties as antioxidants, anti-microbial and cytotoxic agents. Front Pharmacol. 2023;14. <https://doi.org/10.3389/fphar.2023.1084181>
15. Habiban AMA, Mahmoud WA, Kareem TA. Preparation and Characterization of Some Metal Complexes with Heterocyclic Azo Ligand (4-SuBAI). Vol. 12, Baghdad Science Journal Vol.
16. Shih MH, Ke FY. Syntheses and evaluation of antioxidant activity of sydnonyl substituted thiazolidinone and thiazoline derivatives. Bioorg Med Chem. 2004 Sep 1;12(17):4633–43. <https://doi.org/10.1016/j.bmc.2004.06.033>
17. Hasan HA, Alwan WM, Ahmed RM, Yousif EI. Synthesis and Characterization of Some Mixed-Ligand Complexes Containing Azo Dye and 1,10-phenanthroline with Co II , Zn II , Cd II and Hg II Ions. Vol. 28, & Appl. Sci. 2015.
18. Sato H, Beppu I, Haraguchi T, Akitsu T, Parida R, Giri S, et al. Optical properties of chiral Schiff base Mn II , Co II , Ni II complexes having azobenzene †. Vol. 95, J. Indian Chem. Soc. 2018.
19. Kadhim AA, Kareem IK, Ali AAM. Synthesis and Spectral Identification of New Azo-Schiff Base Ligand Derivative from Aminobenzylamine and its Novel Metal Complexes with Cu(II), Zn(II) and

- Hg(II). International Journal of Drug Delivery Technology. 2022 Jan 1;12(1):150–6.
20. Jabbar AI, Al-Jibouri MN, Ismail AH. Synthesis and Structural Studies of Transition Metals Complexes with Poly dentate Azo dye ligand Derived from Coumarine. Egypt J Chem. 2021 Nov 1;64(11):6481–5. [10.21608/EJCHEM.2021.78215.3826](https://doi.org/10.21608/EJCHEM.2021.78215.3826)
21. Bagheri M, Validi M, Gholipour A, Makvandi P, Sharifi E. Chitosan nanofiber biocomposites for potential wound healing applications: Antioxidant activity with synergic antibacterial effect. Bioeng Transl Med. 2022 Jan 1;7(1).
<https://doi.org/10.1002/btm2.10254>
22. V. V. Vaidya. The effects of heavy metal contamination on antioxidant enzyme activity and oxidative stress in the earthworm *Perionyx excavates*. Uttar Pradesh Journal of Zoology. 2023;59–65. [10.56557/upjoz/2023/v44i33421](https://doi.org/10.56557/upjoz/2023/v44i33421)